

16. K. Hegetschweiler, H. Schmalte, H. M. Streit, W. Schneider, *Inorg. Chem.* **29**, 3625 (1990).
17. K. Hegetschweiler *et al.*, *ibid.* **31**, 1299 (1992).
18. V. W. Day and W. G. Klemperer, *Science* **228**, 533 (1985).
19. G. D. Watt, R. B. Frankel, G. C. Papaefthymiou, *Proc. Natl. Acad. Sci. U.S.A.* **82**, 3640 (1985).
20. Theoretical calculations and recent experimental observations support the onset of magnetic ordering effects in exchange-coupled atomic or molecular globular clusters containing more than ten strongly interacting spins [see (24)].
21. T. G. St. Pierre *et al.*, *Biochim. Biophys. Acta* **870**, 127 (1986).
22. The transition from quadrupolar to magnetically split absorption spectra at a particular iron site occurs when the Larmor precession frequency, ν_L , of the nuclear spin of the first excited state of the ^{57}Fe nucleus equals that of the spin fluctuation frequency, ν_s . The local spins in **1** are antiferromagnetically coupled with their neighbors, so they must fluctuate in unison and ν_s is the same for every iron site. Fluctuations of the total spin of the cluster between easy directions of magnetization within the nanocrystalline solid are thermally activated, so the value of ν_s decreases with temperature. Since ν_L is proportional to the local hyperfine field, H_{hf} , the transition from a paramagnetic to a magnetically split spectrum occurs at lower temperatures with smaller H_{hf} . Correspondingly, the ferrous subcomponents of **1**, with decreased H_{hf} as compared to the ferric nuclei, exhibit lower blocking temperatures.
23. M. B. Robin and P. Day, *Adv. Inorg. Chem. Radiochem.* **10**, 247 (1967).
24. G. C. Papaefthymiou, *Phys. Rev. B* **46**, 10366 (1992), and references therein.
25. S. M. Gorun, G. C. Papaefthymiou, R. B. Frankel, S. J. Lippard, *J. Am. Chem. Soc.* **109**, 3337 (1987).
26. W. Micklitz *et al.*, manuscript in preparation.
27. J.-F. You, G. C. Papaefthymiou, R. H. Holm, *J. Am. Chem. Soc.* **114**, 2697 (1992).
28. F. C. Meldrum, B. R. Heywood, S. Mann, *Science* **257**, 522 (1992).
29. R. F. Ziolo *et al.*, *ibid.*, p. 219.
30. P. J. Artymiuk *et al.*, in *Iron Biominerals*, R. B. Frankel and R. P. Blakemore, Eds. (Plenum, New York, 1991), pp. 269–294.
31. V. J. Wade *et al.*, *J. Mol. Biol.* **221**, 1443 (1991).
32. D. M. Lawson *et al.*, *Nature* **349**, 541 (1991).
33. E. R. Bauminger, P. M. Harrison, D. Hechel, I. Nowik, A. Treffy, *Biochim. Biophys. Acta* **1118**, 48 (1991).
34. C.-Y. Yang, A. Meagher, B. H. Huynh, D. E. Sayers, E. C. Theil, *Biochemistry* **26**, 497 (1987).
35. P. M. Hanna, Y. Chen, N. D. Chasteen, *J. Biol. Chem.* **266**, 886 (1991).
36. D. Jacobs, G. D. Watt, R. B. Frankel, G. C. Papaefthymiou, *Biochemistry* **28**, 9216 (1989).
37. D. M. Kurtz, Jr., *Chem. Rev.* **90**, 585 (1990).
38. L. Que, Jr., and A. E. True, *Prog. Inorg. Chem.* **38**, 97 (1990).
39. A. Treffy, J. Hirtzmann, S. J. Yewdall, P. M. Harrison, *FEBS Lett.* **302**, 108 (1992).
40. R. Fischer, *J. Appl. Crystallogr.* **18**, 258 (1985).
41. K. L. Taft *et al.*, in preparation.
42. Supported by the National Institutes of Health, the National Science Foundation, and the Office of Naval Research. K.L.T. acknowledges the National Science Foundation for a Graduate Research Fellowship. We thank H.-C. zur Loye and D. M. Giaquinta for helpful discussions and assistance in the production of Fig. 2, which was prepared by using the program STRUPLO (40).

20 August 1992; accepted 16 November 1992

Identification of a Second Dynamic State During Stick-Slip Motion

Hisae Yoshizawa, Patricia McGuiggan, Jacob Israelachvili*

Stick-slip, or interrupted, motion rather than smooth uninterrupted motion occurs in many different phenomena such as friction, fluid flow, material fracture and wear, sound generation, and sensory "texture." During stick-slip, a system is believed to undergo transitions between a static (solid-like) state and a kinetic (liquid-like) state. The stick-slip motion between various types of pretreated surfaces was measured, and a second, much more kinetic state that exhibits ultra-low friction was found. Transitions to and from this superkinetic state also give rise to stick-slip motion but are fundamentally different from conventional static-kinetic transitions. The results here suggest practical conditions for the control of unwanted stick-slip and the attainment of ultra-low friction.

Recent experiments (1–4) and computer simulations (5–8) have revealed that molecules at the interface between two sliding surfaces can have properties quite unlike their bulk properties. For example, simple liquids can undergo abrupt freezing-melting transitions during sliding (2), a phenomenon that has been shown to result in "stick-slip" friction (6, 7), which is the major cause of damage to moving surfaces. The ability to produce durable low-friction surfaces and lubricant fluids has become an

important factor in the miniaturization of moving components in many technological devices. These include magnetic storage and recording systems (computer disk heads), miniature motors, and many aerospace components. The success of these new materials depends on the production of moving surfaces that exhibit low friction (friction coefficients below 0.01) and smooth motion with no stick-slip. Stick-slip motion, however, is a much more common phenomenon (9, 10–18) and is central to understanding earthquakes (14) and granular flows (13, 17).

Although the underlying physical processes are probably different in each case, most stick-slip phenomena exhibit some

common features, such as an increased stick-slip frequency at higher shear rates and the disappearance of stick-slip above some critical velocity (2, 6, 7, 9–12). For this reason, theoretical models of these phenomena are usually similar (6, 7, 11–14). Thus, the existence of two states has become increasingly accepted: a "static," or solid-like, state, and a "kinetic," or fluid-like, state. In addition, the occurrence of stick-slip motion indicates that the system makes periodic transitions between these two states. Experimental and theoretical studies of liquid films (1, 2, 6, 7) and polymer fluids (10, 18) further show that the transition from stick to slip is analogous to a freezing-melting transition, which occurs when the applied shear stress reaches some critical value at which the solid-like order collapses into a disordered or liquid-like state. During the rapid slip, the elastic potential energy that was stored in the supporting material during the stick phase is transformed into kinetic energy (9). As slip proceeds, the two surfaces decelerate at a rate that depends on the inertial mass of the supporting material (7). This slowing occurs until the relative velocity of the two surfaces is small enough to allow the interfacial region to solidify again, after which the stick-slip cycle is repeated (6). Robbins and Thompson (7) have proposed that this critical velocity is given by

$$v_c \approx C\sqrt{\sigma F_s/M} \quad (1)$$

where F_s is the static friction force, σ is a characteristic molecular or lattice dimension, M is the mass of the supporting material, or stage, and C is a constant close to 0.05. If the shearing velocity v_c is high enough, the interfacial region never solidifies, there is no stick-slip, and the two surfaces continue to move smoothly in the more fluid-like, kinetic state. The static and kinetic frictions are determined and measured solely by the properties of the shearing surfaces but only if sliding proceeds smoothly in one of those states. However, stick-slip behavior reflects transitions between any two states whose frequency, amplitude and critical velocity depend on the inertial and elastic properties of the system (moving machine component or measuring instrument). For example, in the case of interfacial sliding v_c depends directly on the inertia of the stage (Eq. 1). As a corollary to Eq. 1, Robbins and colleagues (19) have also found that the slip length is proportional to the inverse of the elastic stiffness of the system, which is equivalent to the constant of the spring that is used to measure the friction force in a surface forces apparatus (SFA).

A standard SFA (20) that was modified for shear studies (1, 2, 15) was used in the friction force experiments described here.

Department of Chemical and Nuclear Engineering and Materials Department, University of California, Santa Barbara, CA 93106.

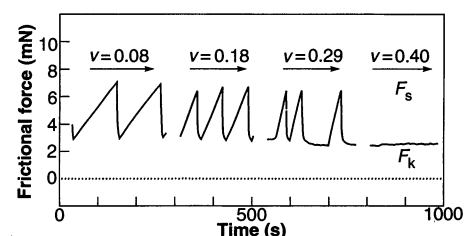
*To whom correspondence should be addressed.

The friction SFA is based on the pin-on-flat method (9), where two smooth surfaces can be moved toward or away from each other as well as slid (sheared) laterally past each other. Sliding is affected by moving a stage of mass $M = 20$ g horizontally at some fixed velocity, v . This stage is coupled to one of the surfaces with a spring that measures the friction force: the spring's deflection during motion gives the friction force, F (1, 2). In these studies, we used a variety of untreated and surfactant-coated mica surfaces. The latter are particularly suitable for such studies because they can be transformed into well-characterized, molecularly smooth surfaces with a wide range of surface molecular configurations: solid, crystalline, amorphous, fluid-like, and liquid-like (21). In addition, surfactant monolayers have long been used as boundary lubricants to reduce the friction and wear of surfaces (22), although their tribological behavior at the molecular level is still not fully understood (23). We describe our results first for untreated mica surfaces across a thin hydrocarbon liquid film and then for surfactant-coated surfaces that have the same molecules end-attached to them.

Figure 1 shows friction traces that are typical when two molecularly smooth surfaces of mica slide past each other while separated by molecularly thin films of hexadecane. The stick-slip is of the conventional static-kinetic type and disappears above some critical shearing velocity, $v_c \approx 0.4 \mu\text{m s}^{-1}$. Qualitatively similar experimental results have been obtained with many other liquid-like systems (1, 2, 15). In addition, recent computer simulations have satisfactorily explained this type of stick-slip in terms of freezing-melting cycles of the confined liquid films (6, 7) and have provided a relation between v_c and other properties of the system as expressed by Eq. 1. Thus, with the values, $F_s = 6$ mN, $\sigma = 0.4$ nm (the hydrocarbon chain diameter), $M = 20$ g (the mass of the supporting stage), and $C = 0.05$ inserted in Eq. 1, we obtain $v_c \approx 0.5 \mu\text{m s}^{-1}$, which is close to the measured critical velocity of $\sim 0.4 \mu\text{m s}^{-1}$.

We also obtained friction traces with two surfactant monolayer-coated mica surfaces (Fig. 2). Each layer is composed of hexadecyl chains that are attached at one end to the mica surface (in contrast to the free hexadecane chains of Fig. 1). The results show that, in addition to transitions between the static and kinetic states at low shear rates ($v \ll 0.1 \mu\text{m s}^{-1}$), another stick-slip regime appears at much higher velocities ($v_c^* > 0.3 \mu\text{m s}^{-1}$). Increases in the temperature and the relative humidity reduced v_c^* and facilitated transitions to this more kinetic state (inset, Fig. 2), probably because the changes in these factors help soften the monolayers (24). The phenom-

Fig. 1. Exact reproductions of chart recorder traces of the friction force of a hexadecane ($\text{C}_{16}\text{H}_{34}$) film between two shearing mica surfaces at increasing sliding velocities, v (in micrometers per second). A modified (SFA) (1, 2) was used that allows for simultaneous measurements of the normal applied load (L), the contact area (A), the applied pressure ($P = L/A$), the thickness of the liquid film (D), and the shear rate ($\tau = v/D$) between the two sliding surfaces. Experimental conditions: $L = 11.2 \times 10^{-3}$ N, $A = 4.3 \times 10^{-9}$ m², $P = L/A = 2.6 \times 10^6$ N m⁻², $D = 0.4$ to 0.8 nm, $v = 0.08$ to $0.4 \mu\text{m s}^{-1}$ ($\tau \approx 10^3$ s⁻¹); the atmosphere was dry N_2 gas [relative humidity (RH) = 0%] and $T = 18^\circ\text{C}$. With increasing v , the stick-slip spikes generally increase in frequency and decrease in magnitude. As the critical sliding velocity v_c is approached, the spikes become erratic and eventually disappear at $v = v_c$ (2, 6, 7). At higher values of v the sliding continues smoothly in the kinetic state. In this system, the static friction coefficient was $\mu_s = \text{static force of friction } (F_s)/L = 0.5$, the kinetic friction coefficient was $\mu_k = \text{the kinetic force of friction } (F_k)/L = 0.25$, and $v_c \approx 0.4 \mu\text{m s}^{-1}$, which corresponds to a critical shear rate of $\tau_c = v_c/D \approx 10^3$ s⁻¹.



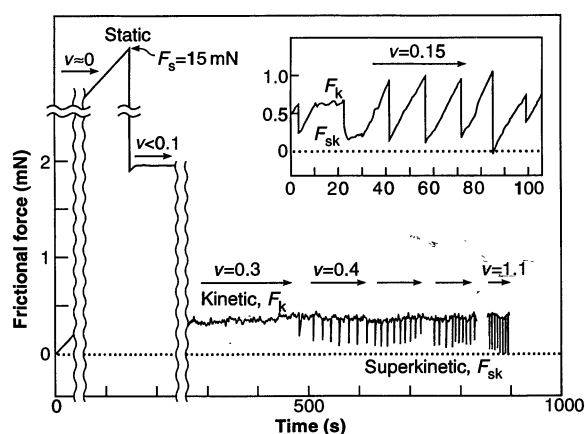
enon of two distinct stick-slip regimes that occur in the same system has not been observed with the free hydrocarbon liquids or with any other liquid studied, nor has it been reported in other tribological or non-tribological systems. However it may have been observed unknowingly.

On closer scrutiny, one finds that the stick-slip transitions that occur at higher sliding speeds (type II) are quite different from the conventional static-kinetic transitions (type I). The most striking difference is that type II spikes are all "inverted," falling below the smooth kinetic friction base line rather than rising above it, as is generally observed with type I transitions (Fig. 1) (2, 6, 15). A number of other experimental observations further indicate that type II stick-slip is fundamentally different from normal static-kinetic stick-slip: (i) Type I stick-slip always disappears above some critical velocity; that of type II always appears above some critical velocity; (ii) type I stick-slip can be made to disappear with

increasing load and type II comes in above some critical load; and (iii) type II stick-slip has only been seen with surfactant boundary layer lubricants but not with other surfaces, whether unlubricated or liquid-lubricated (1, 2, 15). Another, more qualitative observation is that during type II stick-slip the friction falls to much lower values than during conventional type I stick-slip.

The data in Fig. 2 suggest that with increasing velocity the system starts to make transitions from the kinetic state, which already exhibits a low friction coefficient of 0.01 to 0.03, to an even more kinetic state that exhibits ultralow friction with coefficients well below 0.01. During slips to the superkinetic state, the friction often falls transiently to, or even below, zero. This "negative" friction force should not be construed as a steady-state negative friction coefficient, which is thermodynamically impossible, but rather is a transient overshoot that arises from the finite inertial damping of the surfaces and their support. Thus, if the

Fig. 2. Measured friction traces at increasing v (in micrometers per second) of end-attached hydrocarbon chains on mica under similar sliding conditions to those in Fig. 1. Double-chained surfactant monolayers of DHDA⁺ [(C₁₆H₃₃)₂-(C₂H₆N⁺)] were deposited on mica surfaces as described in (2, 24). The positively charged headgroups of the DHDA⁺ molecules adhere strongly to the negatively charged mica surfaces and did not come off during sliding. Experimental conditions: monolayer coverage was $35 \pm 5 \text{ \AA}^2$ per hydrocarbon chain, $D = 3.6$ nm, $L = 19$ to 31 mN, and $A = 3.6$ to 6.0×10^{-9} m². Conditions in main figure ($T = 25^\circ\text{C}$, RH = 0%): $v_c < 0.01 \mu\text{m s}^{-1}$ (only one static-kinetic stick-slip spike is shown on the far top left), $v_c^* \approx 0.4 \mu\text{m s}^{-1}$, $\mu_s = F_s/L = 14.6 \times 10^{-3}/19.3 \times 10^{-3} = 0.75$, $\mu_k = F_k/L = 0.4 \times 10^{-3}/28 \times 10^{-3} = 0.015$, and the superkinetic friction coefficient $\mu_{sk} = F_{sk}/L \approx 0.003$. Conditions in inset ($T = 29^\circ\text{C}$, RH = 100%): $v_c^* \approx 0.1 \mu\text{m s}^{-1}$, $\mu_k = 1.0 \times 10^{-3}/30 \times 10^{-3} = 0.03$, $\mu_{sk} = 0.005$. Note the extended sliding, with some noise, both in the kinetic state (for ~ 15 s) and in the superkinetic state (for ~ 10 s).



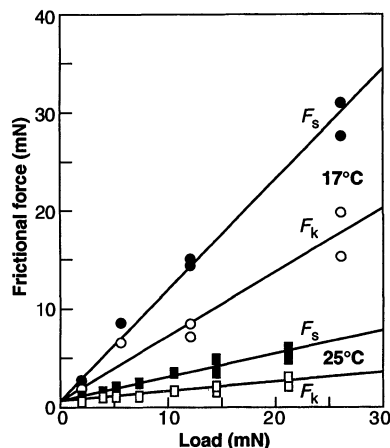


Fig. 3. Effect of temperature on F_s and F_k of a free hexadecane film between two mica surfaces. Experimental conditions were similar to those of Fig. 1, with $v = 0.4 \mu\text{m s}^{-1}$; at 17°C , $\mu_s = 1.0$ and $\mu_k = 0.7$; and at 25°C , $\mu_s = 0.25$ and $\mu_k = 0.1$.

transition from kinetic to superkinetic states is triggered by the sudden drop in friction force from F_k to a much smaller F_{sk} , then during the slip the measured friction will, depending on the mechanical damping of the system, fall directly to a new steady-state value at F_{sk} , slip momentarily below F_{sk} before equilibrating at F_{sk} , or slip and then immediately stick again to return to the kinetic state at F_k . The inset to Fig. 2 shows examples of all three types of phenomena. To eliminate the possibility that extraneous mechanical vibrations in the apparatus caused the observed effects, we mention that similar (type II) stick-slip friction is measured when a nonmechanical piezoelectric-bimorph stage is used (25). In addition, the friction is strongly influenced by changes in the relative humidity, temperature, and type of boundary lubricant layer used (25), although none of these factors affects the mechanical properties of the apparatus.

Temperature-dependent studies revealed further systematic differences between the two types of stick-slip. Figure 3 shows how the static and kinetic frictions of a free (unanchored) liquid hexadecane film vary with applied load at two different temperatures. The data conform to the expected behavior for normal stick-slip: The friction increases roughly linearly with increasing load (Amontons' law) and decreases with increasing temperature. The latter trend is due to the increased fluidity and mobility of the hydrocarbon molecules as temperature increases, which results in a reduced friction similar to the reduced viscosity of a liquid at higher temperatures.

In contrast (Fig. 4), over the same temperature range the stick-slip friction of the anchored molecules is quite different: The kinetic friction increases with increasing

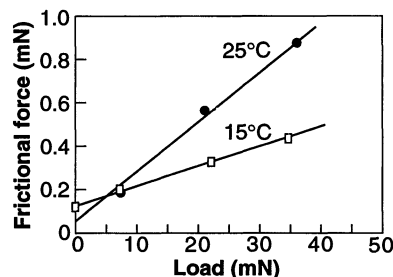


Fig. 4. Effect of temperature on F_k of a surfactant film of $\text{CTA}^+ [\text{C}_{16}\text{H}_{33} - \text{N}(\text{CH}_3)_3]^+$ between two mica surfaces. Experimental conditions were similar to those of Fig. 2, with $v = 0.2 \mu\text{m s}^{-1}$ and $\text{RH} = 0\%$. At 15°C , $\mu_k = 0.012$, and at 25°C , $\mu_k = 0.025$. The superkinetic friction is not shown because it was close to zero at all loads (Fig. 2) and was too small to be measured accurately.

temperature, whereas the superkinetic friction remains small at all temperatures and loads. The increase in friction with temperature is particularly unexpected. Furthermore, on the basis of previous studies of polymer and hydrocarbon chain interdigitation effects (21), this increase suggests that the higher temperature allows for greater hydrocarbon chain interdigitation to occur (by way of interdiffusion or reptation) across the interface, which enhances the frictional forces (25). This interpretation further suggests that in the kinetic state the chains within the film are not in a true liquid state but in some gel-like or ductile glassy state where chain reconfigurations are highly restricted and occur much more slowly than in the bulk liquid (4, 8).

When studied over a limited range of experimental conditions, the inverted stick-slip pattern characteristic of kinetic-superkinetic transitions (Fig. 2) may often be indistinguishable from static-kinetic stick-slip (Fig. 1). Superkinetic stick-slip may therefore occur in many systems where normal stick-slip has been reported. A number of experimental studies have shown that end-attached hydrocarbon or polymer chains perform as better boundary lubricants than unbound chains (free liquid films) (26, 27). Their behavior may be due to superkinetic sliding at the shearing asperity junctions. In addition, the ultra-low friction we have measured occurs without a liquid lubricant and at high loads. Thus, this condition is quite different from situations in which a repulsive force between two surfaces in a liquid keeps them apart (20), resulting in a large gap thickness and low friction.

As we consider the possible molecular configurations in a thin film during superkinetic sliding, our results show that this "shear-thinning" effect is not gradual, as in bulk polymer (18) or colloidal (28) systems. Moreover, it involves a discontinuous transition, probably between a disordered kinetic

state that exhibits normal friction and a more ordered state that exhibits ultra-low friction. From our limited results, it appears that this effect can arise only when the sheared molecules are functionally end-attached to each surface. This process is probably required for the molecules to become uniformly shear-aligned, as each layer is "combed" by the other. In contrast, unattached molecules, or attached molecules at low shear rates ($v < v_c^*$), that remain interdigitated or entangled within the film, retain a higher resistance to motion when sliding in the kinetic state. Furthermore, many thermotropic and lyotropic liquid crystal films exhibit lower friction in the more ordered, smectic or lamellar states than in the more disordered, and therefore more entangled, nematic or isotropic states (29). One may further speculate that because liquid crystals and surfactant monolayers have a large variety of different equilibrium phase states (30) other types of "dynamic" phase states may also exist.

The idea of some superkinetic but ordered state may seem contradictory: that of a fluid becoming more compact and ordered, and thus more solid-like from a structural aspect, but flowing more easily and thus becoming more liquid-like from a dynamic aspect. The physical or molecular mechanisms that underlie this type of dynamic phase transition have not been investigated because the high shear rates required are rarely encountered in practice in bulk complex-fluid systems. However, high shear rates are commonly attained at the interface between two shearing surfaces because the entire velocity gradient occurs across a film of molecular dimensions. Thus, what may be a rare phenomenon in bulk flow may be common at interfaces.

REFERENCES AND NOTES

1. J. N. Israelachvili, P. M. McGuiggan, A. M. Homola, *Science* **240**, 189 (1988).
2. M. L. Gee, P. M. McGuiggan, J. N. Israelachvili, A. Homola, *J. Chem. Phys.* **93**, 1895 (1990).
3. J. Van Alsten and S. Granick, *Phys. Rev. Lett.* **61**, 2570 (1988); *Macromolecules* **23**, 4856 (1990).
4. H. W. Hu, G. A. Carson, S. Granick, *Phys. Rev. Lett.* **66**, 2758 (1991); J. Van Alsten and S. Granick, *Langmuir* **6**, 876 (1990).
5. M. Schoen, J. H. Cushman, D. J. Diestler, C. L. Rhykerd, *J. Chem. Phys.* **88**, 1394 (1988); M. Schoen, C. L. Rhykerd, D. J. Diestler, Jr., J. H. Cushman, *Science* **245**, 1223 (1989).
6. P. A. Thompson and M. O. Robbins, *Science* **250**, 792 (1990).
7. M. O. Robbins and P. A. Thompson, *ibid.* **253**, 916 (1991).
8. P. A. Thompson, G. S. Grest, M. O. Robbins, *Phys. Rev. Lett.* **68**, 3448 (1992).
9. E. Rabinowicz, *Friction and Wear of Materials*, (Wiley, New York, 1965), chap. 4.
10. M. M. Denn, *Annu. Rev. Fluid Mech.* **22**, 13 (1990); C. S. Campbell, *ibid.*, p. 57.
11. G. M. McLelland, in *Adhesion and Friction*, M. Grunze and H. J. Kreuzer, Eds., vol. 17 of Springer Series in Surface Science (Springer, Berlin, 1989), pp. 1-16.
12. D. Landheer and A. W. J. de Gee, *MRS Bull.* **XVI** (no. 10) (1991), p. 36.

13. P. A. Thompson and G. S. Grest, *Phys. Rev. Lett.* **67**, 1751 (1991).
14. J. M. Carlson and J. S. Langer, *ibid.* **62**, 2632 (1989).
15. S. J. Hirz *et al.*, *Langmuir* **8**, 328 (1992).
16. W. B. Russel, D. A. Saville, W. R. Schowalter, *Colloidal Dispersions* (Cambridge Univ. Press, Cambridge, 1989), chap. 14.
17. H. M. Jaeger and S. R. Nagel, *Science* **255**, 1523 (1992).
18. H. A. Barnes, J. F. Hutton, K. Walters, *An Introduction to Rheology* (Elsevier, Amsterdam, 1989); R. L. Hoffman, *J. Colloid Interface Sci.* **46**, 491 (1974).
19. M. O. Robbins and P. A. Thompson, personal communication.
20. J. N. Israelachvili, *Intermolecular and Surface Forces* (Academic Press, London, ed. 2, 1991).
21. Y. L. Chen, C. Helm, J. N. Israelachvili, *J. Phys. Chem.* **95**, 10736 (1991).
22. F. P. Bowden and D. Tabor, *Friction and Lubrication* (Methuen, London, 1967), chap. 9.
23. B. J. Briscoe, D. C. B. Evans, D. Tabor, *J. Colloid Interface Sci.* **61**, 9 (1977).
24. Y. L. Chen *et al.*, *J. Phys. Chem.* **93**, 7057 (1989).
25. Y. L. Chen, H. Yoshizawa, J. Israelachvili, unpublished results.
26. M. Suzuki, Y. Saotome, M. Yanagisawa, *Thin Solid Films* **160**, 453 (1988).
27. E. Ando *et al.*, *ibid.* **180**, 287 (1989).
28. B. J. Ackerson and N. A. Clarke, *Physica A* **118**, 221 (1983); W. Xue and G. S. Grest, *Phys. Rev. Lett.* **64**, 419 (1990); M. J. Stevens, M. O. Robbins, J. F. Belak, *ibid.* **66**, 3004 (1991).
29. G. Bireslaw, *Tribology and the Liquid-Crystalline State*, ACS Symposium Series No. 441 (American Chemical Society, Washington, DC, 1990).
30. A. M. Bibo, C. M. Knobler, I. R. Peterson, *J. Phys. Chem.* **95**, 5591 (1991).
31. Supported by the U.S. Department of Energy and Exxon Chemicals. We thank S. Banerjee, G. Fredrickson, S. Granick, J. Langer, G. Leal, D. Pearson, M. Robbins, and P. Thompson for insightful comments and discussions.

29 June 1992; accepted 30 November 1992

Three-Dimensional Instabilities of Mantle Convection with Multiple Phase Transitions

S. Honda, D. A. Yuen, S. Balachandar, D. Reuteler

The effects of multiple phase transitions on mantle convection are investigated by numerical simulations that are based on three-dimensional models. These simulations show that cold sheets of mantle material collide at junctions, merge, and form a strong downflow that is stopped temporarily by the transition zone. The accumulated cold material gives rise to a strong gravitational instability that causes the cold mass to sink rapidly into the lower mantle. This process promotes a massive exchange between the lower and upper mantles and triggers a global instability in the adjacent plume system. This mechanism may be cyclic in nature and may be linked to the generation of superplumes.

Phase transitions in the mantle may affect the amount of flow between the upper and lower mantles (1, 2). Recently, the effects of phase transitions on mantle convection have been studied with the use of numerical models (3-7), but most have been restricted to two dimensions. Some interesting phenomena, such as the intermittently layered convection that is enforced by the spinel-to-perovskite phase transition (3-5), have been shown in these studies. The generation of diapirs in the upper mantle has also been demonstrated (4). Three-dimensional (3-D) studies are needed to confirm these interesting 2-D findings. Seismic tomographic studies (8, 9) have indicated that slabs may be lying horizontally along the phase transition zone. Investigations in two dimensions (4, 6, 7) have also shown the importance of including the second phase transition, olivine to spinel, at a depth of 400 km. In this report, we present results from 3-D numerical simulations of mantle convection with both major phase transitions and discuss an instability

in convection that is produced by the phase transitions. This instability may help ex-

plain the correlation between subduction rate changes and the superplume events (10) that occurred 120 million years ago and led to the unusually rapid production of the oceanic crust and the stabilization of the polarity of the Earth's magnetic field. The instability bears no resemblance to local boundary-layer instabilities that are seen in models of convection without phase changes. This global instability, which is produced by phase transitions, was first observed in 2-D models (6, 7), but these 3-D simulations have confirmed their existence.

The model that we used is based on a Cartesian geometry with an aspect ratio of 5 by 5 by 1, with unity being the depth of the layer. A mantle depth of 2000 km is assumed in which the two major

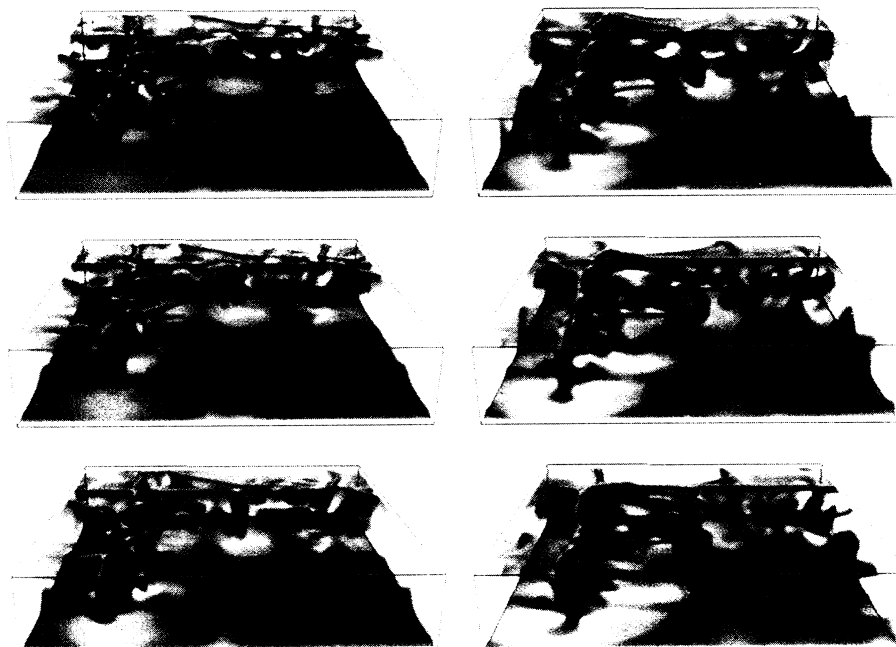


Fig. 1. Sequence of snapshots of temperature T . Sequence of events begins with the top left panel, goes down the column and continues with the right column, going down at equal time intervals. The first and last frames represent $t = 0.010$ (1.270 billion years) and $t = 0.0125$ (1.588 billion years). Cold and hot anomalies have been volume-rendered in blue and yellow hues, respectively, as indicated by the color bar. The void represents values close to the average value of 0.5. The aspect ratio of this 3-D box is 5 by 5 by 1.

S. Honda, Department of Earth and Planetary Systems Science, University of Hiroshima, Higashi-Hiroshima 724, Japan.

D. A. Yuen and D. Reuteler, Minnesota Supercomputer Institute and Department of Geology and Geophysics, University of Minnesota, Minneapolis, MN 55415.

S. Balachandar, Department of Theoretical and Applied Mechanics, University of Illinois, Urbana, IL 61801.